HHS Public Access

Author manuscript

Cell Rep. Author manuscript; available in PMC 2021 August 17.

Published in final edited form as:

Cell Rep. 2020 April 14; 31(2): 107494. doi:10.1016/j.celrep.2020.03.058.

Immunotherapeutic Blockade of CD47 Inhibitory Signaling Enhances Innate and Adaptive Immune Responses to Viral Infection

Lamin B. Cham[1], **Laughing Bear Torrez Dulgeroff**[2], **Michal Caspi Tal**[2], **Tom Adomati**[1], **Fanghui Li**[1], **Hilal Bhat**[1], **Anfei Huang**[3], **Philipp A. Lang**[3], **Mary E. Moreno**[4], **Jose M. Rivera**[4], **Sofiya A. Galkina**[4], **Galina Kosikova**[4], **Cheryl A. Stoddart**[4], **Joseph M. McCune**[4,6], **Lara M. Myers**[5], **Irving L. Weissman**[2], **Karl S. Lang**[1,*], **Kim J. Hasenkrug**[5,7,*]

[1]Institute of Immunology, Medical Faculty, University of Duisburg-Essen, Hufelandstrasse 55, 45147 Essen, Germany

[2]Institute for Stem Cell Biology and Regenerative Medicine, and Ludwig Center for Cancer Stem Cell Research, Stanford University School of Medicine, Stanford, CA 94305, USA

[3]Department of Molecular Medicine II, Medical Faculty, Heinrich Heine University, 40225 Dusseldorf, Germany

[4]Department of Medicine, Division of Experimental Medicine, University of California, San Francisco, CA 94110, USA

[5]Laboratory of Persistent Viral Diseases, Rocky Mountain Laboratories, NIAID, NIH, Hamilton, MT 59840, USA

[6]Present address: HIV Frontiers/Global Health Innovative Technology Solutions, Bill & Melinda Gates Foundation, Seattle, WA 98109, USA

[7]Lead Contact

SUMMARY

Paradoxically, early host responses to infection include the upregulation of the antiphagocytic molecule, CD47. This suggests that CD47 blockade could enhance antigen presentation and subsequent immune responses. Indeed, mice treated with anti-CD47 monoclonal antibody

*Correspondence: karlsebastian.lang@uk-essen.de (K.S.L.), khasenkrug@nih.gov (K.J.H.).

AUTHOR CONTRIBUTIONS

Conceptualization: K.J.H., I.L.W., L.B.C., J.M.M., and C.A.S.; Methodology, K.J.H., L.M.M., L.B.C., K.S.L., M.C.T., L.B.T.D., and C.A.S.; Investigation, L.B.C., T.A., F.L., H.B., A.H., P.A.L., M.E.M., J.M.R., S.A.G., and G.K.; Verification, L.B.C., K.J.H., and C.A.S.; Formal Analysis, L.B.C., K.J.H., L.B.T.D., and M.E.M.; Resources, K.S.L., C.A.S., and K.J.H.; Writing – Original Draft, L.B.C., K.J.H., and L.B.T.D.; Writing – Review & Editing, L.B.C., K.J.H., L.B.T.D., M.C.T., J.M.M., I.L.W., C.A.S., and K.S.L.; Visualization, K.J.H., L.B.C., L.B.T.D., M.C.T., and C.A.S.; Resources, K.S.L., K.J.H., and C.A.S.; Supervision, K.S.L., K.J.H., and C.A.S.; Project Administration, K.J.H., K.S.L., C.A.S., and L.B.C.; Funding Acquisition, K.S.L., K.J.H., and C.A.S.

SUPPLEMENTAL INFORMATION

Supplemental Information can be found online at https://doi.org/10.1016/j.celrep.2020.03.058.

DECLARATION OF INTERESTS

K.J.H., C.A.S., J.M.M., and I.L.W. are listed as inventors on US patent 2019/0092873 A1 CD47 Targeted Therapies for the Treatment of Infectious Disease. I.L.W. is a co-founder, director, and stockholder in Forty Seven, Inc., a public company involved in CD47-based immunotherapy of cancer.

following lymphocytic choriomeningitis virus infections show increased activation of both macrophages and dendritic cells (DCs), enhancement of the kinetics and potency of $CD8^+$ T cell responses, and significantly improved virus control. Treatment efficacy is critically dependent on both APCs and $CD8^+$ T cells. In preliminary results from one of two cohorts of humanized mice infected with HIV-1 for 6 weeks, CD47 blockade reduces plasma p24 levels and restores $CD4^+$ T cell counts. The results indicate that CD47 blockade not only enhances the function of innate immune cells but also links to adaptive immune responses through improved APC function. As such, immunotherapy by CD47 blockade may have broad applicability to treat a wide range of infectious diseases.

Graphical Abstract

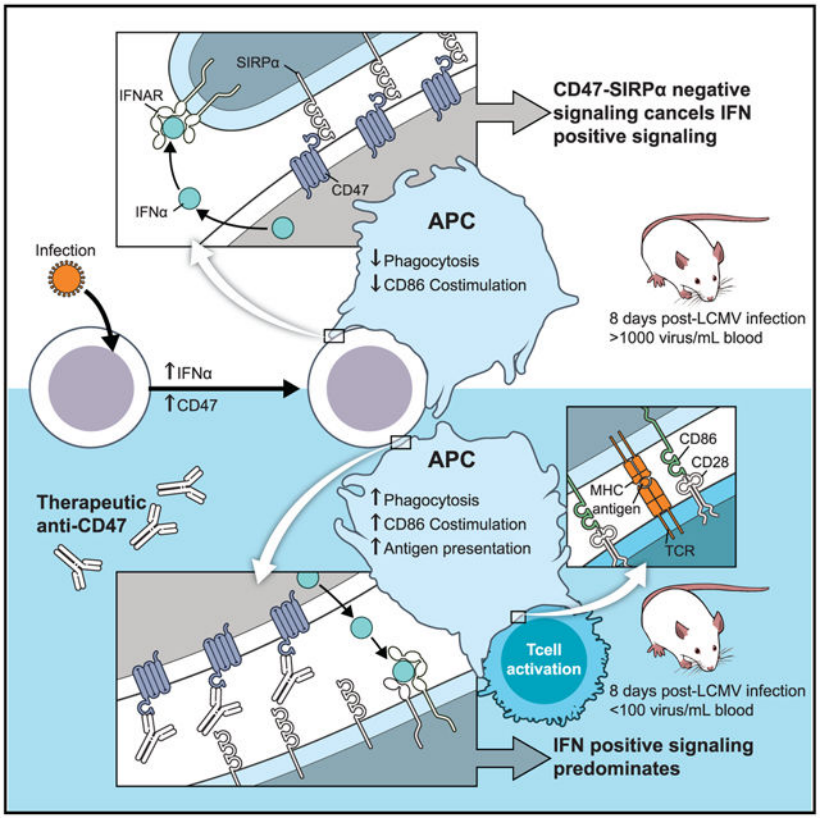

In Brief

Cham et al. describe a way to enhance natural immune responses to infections by blocking interactions between two molecules (CD47 and SIRPα) that normally put brakes on the immune system. Since this therapy targets the immune system, it could have broad applicability against a wide range of infectious agents.

INTRODUCTION

Integrin-associated protein (IAP), also known as CD47, is a ubiquitously expressed glycoprotein of the immunoglobulin super-family (Barclay and Van den Berg, 2014; Liu

et al., 2017). In the immune system, CD47 interacts with signal regulatory protein-alpha (SIRPα or CD172a), which is expressed on macrophages, dendritic cells (DCs) (Barclay and Van den Berg, 2014), and as recently reported, cytolytic T lymphocytes (Myers et al., 2019). The interaction of CD47 with SIRPα on macrophages and DCs results in an anti-phagocytic ("don't-eat-me") signal as a result of the phosphorylation of immunoreceptor tyrosine-based inhibitory motifs (ITIMs) within the cytoplasmic tail of SIRPα. Such phosphorylation leads to the recruitment and activation of Src homology 2 (SH2) domain-containing phosphatases, SHP-1 and SHP-2, which in turn regulate downstream signaling pathways, usually in an inhibitory manner (Barclay and Van den Berg, 2014). The purpose of this inhibitory signaling is to prevent the phagocytosis of normal, healthy cells. High expression of CD47 on hematopoietic stem cells (HSCs) assures their ability to migrate without being phagocytosed (Jaiswal et al., 2009), while loss of CD47 on aged red blood cells leads to macrophage-mediated programmed cell removal (PrCR) (Bian et al., 2016). There is also evidence that CD47-SIRPα interactions are important contributors to the maintenance of peripheral tolerance via STAT3 activation (Toledano et al., 2013). CD47 also binds to, and acts as a signaling receptor for thrombospondin-1 (TSP-1), a secreted matricellular glycoprotein with important roles in multiple cellular functions including antiangiogenic activity (Isenberg et al., 2006), cell-to-cell adhesion, cell-to-matrix adhesion, proliferation, apoptosis inflammation, and endothelial cell senescence (Sick et al., 2012; Gao et al., 2016). Thus, CD47 can produce complex biological effects, although naive mice with genetic inactivation of the CD47 gene display no obvious phenotypic abnormalities other than a short half-life of their red cells transfused into syngeneic wild-type recipients (Lindberg et al., 1996).

CD47 was first cloned from an ovarian tumor cell (Campbell et al., 1992), and it is now known that all tumor cells upregulate CD47 to evade innate immune clearance (Betancur et al., 2017; Chao et al., 2011; Jaiswal et al., 2009; Majeti et al., 2009). Thus, antibody-mediated CD47 blockade alone or paired with anti-cancer IgG1 antibodies such as rituximab has been pioneered to treat tumors in both animal models (Chao et al., 2010, 2011; Jaiswal et al., 2009; Majeti et al., 2009; Schürch et al., 2019) and in clinical trials (Advani et al., 2018). Mechanistic studies in mice have demonstrated that the anti-tumor effects from antibody-mediated CD47 blockade involve not only enhancement of macrophage-mediated effects, but also macrophage and DC cross-priming of T cell responses that were required for tumor elimination (Liu et al., 2015; Tseng et al., 2013). It was very recently shown that CD47 is upregulated in infected cells as a checkpoint response to pathogen recognition by infected cells and also in uninfected DCs in response to pro-inflammatory cytokine stimuli (M.C.T., L.B.T.D., L.M.M., M. Hasenkrug, L.B.C., K. Mayer-Barber, A.C. Bohrer, E. Castro, Y. Yiu, C. Lopez Angel, E. Pham, A. Carmody, R. Messer, E. Gars, J. Kortmann, M. Markovic, K. Peterson, T. Woods, C. Winkler, D. Wagh, B. Fram, T. Nguyen, D. Corey, R. Sab Kallaru, N. Banaei, J. Rajadas, D. Monack, A. Ahmed, M. Davis, J. Glenn, T.A., K.S.L., K.J.H., and I.L.W., unpublished data). The upregulation of CD47 on DCs suggests that downstream effects on T cell responses might also be occurring, especially in the context of inflammation or infection. Support for the idea that CD47 is acting in an immunosuppressive manner during infections comes from results showing that all pox viruses encode a CD47 mimic (Cameron et al., 2005a; Campbell et al., 1992). The best

studied mimic is that of myxoma virus, which not only downregulates macrophage and T cell activation *in vivo* (Cameron et al., 2005a), but is a potent virulence factor required for *in vivo* virus spread (Cameron et al., 2005b). These findings suggest that antibody-mediated CD47 blockade during viral infection might enhance immunity and lead to quicker virus clearance.

To address this issue, we investigated the immune responses of mice that were treated with anti-CD47 blocking antibodies during infection with the virulent WE strain of lymphocytic choriomeningitis virus (LCMV) (Zapata et al., 2011; Ciurea et al., 1999; Lehmann-Grube, 1971). The WE strain is similar to the Armstrong (Arm) strain in the induction of acute, self-resolving infections that are cleared from C57BL/6 mice in a $CD8^+$ T cell-dependent manner (Fung-Leung et al., 1991) with similar kinetics (Moskophidis et al., 1995). LCMV is a natural pathogen of mice and can cause zoonotic infections in humans with clinical signs ranging from unnoticeable to severe. LCMV has been extensively used as a model pathogen to study basic mechanisms of immunity. We also tested CD47 blockade during established human immunodeficiency virus (HIV-1) infections in SCID-hu mice (McCune et al., 1988) implanted with human fetal liver, thymus, and peripheral lymphoid organs. Our results demonstrate that using anti-CD47 as a therapeutic checkpoint inhibitor significantly improved the host responses to two widely disparate infectious diseases. The mechanisms of action of CD47 blockade suggest broad applicability to an extensive range of infections.

RESULTS

Anti-CD47 Therapy Reduces Virus Loads and Activates Innate and Adaptive Immunity

To determine whether mice infected with LCMV upregulated expression of CD47 as reported for other infectious agents (M.C.T., L.B.T.D., L.M.M., M. Hasenkrug, L.B.C., K. Mayer-Barber, A.C. Bohrer, E. Castro, Y. Yiu, C. Lopez Angel, E. Pham, A. Carmody, R. Messer, E. Gars, J. Kortmann, M. Markovic, K. Peterson, T. Woods, C. Winkler, D. Wagh, B. Fram, T. Nguyen, D. Corey, R. Sab Kallaru, N. Banaei, J. Rajadas, D. Monack, A. Ahmed, M. Davis, J. Glenn, T.A., K.S.L., K.J.H., and I.L.W., unpublished data.), flow cytometry was used to analyze CD47 cell surface expression levels on six different hematopoietic cell subsets: macrophages, DCs, B cells, natural killer (NK) cells, $CD4^+$ T cells, and $CD8^+$ T cells at 3 days post-infection (dpi), the peak of the innate response. Significant upregulation was observed on all subsets (Figure 1A). We next investigated whether blockade of CD47-mediated signaling could affect virus control in mice infected with LCMV. Daily injection of anti-CD47 monoclonal antibody was initiated at 2 days post-LCMV infection and continued for five injections. Virus titers were measured from the blood and kidneys (a site of persistent LCMV-WE; Ciurea et al., 1999) in a kinetic manner. No significant difference in blood viremia was observed at 3 dpi, but by 5 dpi there was significantly lower viremia in the blood of treated mice (Figure 1B). Viremia was cleared to below the level of detection in the blood of all treated mice by 8 dpi, while the mock-treated mice still had a mean titer of 2.8 $\log_{10}$ (Figure 1B). Kidney virus levels in treated mice rose to lower levels than in mock-treated and began to resolve at a faster rate (Figure 1C). The anti-CD47 therapy produced a mean 27-fold reduction in kidney virus compared to mock-treated mice at 10 dpi (Figure 1C).

We next analyzed immunological responses that might be involved in the mechanism of anti-CD47-induced virus control. Flow-cytometric analysis of spleen cells revealed that anti-CD47 therapy significantly increased the activation (CD86 expression) of macrophages by 5 dpi (Figure 1D) and DCs by 3 dpi (Figure 1E). Furthermore, the numbers of splenic $CD4^+$ and $CD8^+$ T cells in anti-CD47-treated mice expanded at a significantly faster rate and to higher levels than controls (Figures 1F and 1G). In treated mice, the LCMV-specific (tetramer$^+$) $CD8^+$ T cells expanded at similar rates but to higher levels (Figure 1H). It is unclear at this time why the overall $CD8^+$ T cell response in anti-CD47-treated mice contracted between days 7 and 10 while the LCMV gp33-specific (Tetramer$^+$) response was higher at 10 dpi than at 7 dpi. At 7 dpi, the peak of $CD8^+$ T cell expansion in the anti-CD47 group, there were higher numbers of recently cytotoxic cells (as measured by cell surface CD107a expression) as well as higher numbers of interferon (IFN)-γ-producing cells, indicating that the $CD8^+$ T cells were functional (Figure 1I). Thus, anti-CD47 treatment was associated with higher activation of antigen-presenting cells (APCs), higher levels of functional $CD8^+$ T cells, and more rapid clearance of LCMV infections.

Efficacy of CD47 Blockade Is Dependent on $CD8^+$ T Cells and APCs

$CD8^+$ T cells are known to play an essential role in the resolution of LCMV infections (Fung-Leung et al., 1991; Lehmann-Grube, 1971), so it was of interest to determine whether they were critical for the efficacy of CD47 blockade. The anti-CD47 treatments were repeated, this time in mice depleted of $CD8^+$ T cells prior to infection. In control animals, anti-CD47 therapy again reduced LCMV plasma virus to below the limit of detection by 8 dpi, but no virus reduction was observed when $CD8^+$ T cells were depleted (Figure 2A). Furthermore, LCMV viremia did not even resolve by 10 dpi in the T cell-depleted group, indicating that the efficacy of CD47 blockade was dependent on $CD8^+$ T cells. In contrast, depletion of $CD4^+$ T cells did not affect CD47 blockade efficacy in reducing viremia, and there was no detectable virus in any of the groups (Figure 2B). Macrophages express high levels of the CD47 receptor (SIRPα) and are known to mediate much of the effect of anti-CD47 during tumor immunotherapy (Gu et al., 2018; Schürch et al., 2019; Vaeteewoottacharn et al., 2019; Weiskopf et al., 2016). Thus, we next used clodronate-loaded liposomes to deplete macrophages *in vivo* prior to infection and observe the effects on $CD8^+$ T cells and virus clearance. Overall, macrophage depletion resulted in a reduction of $CD8^+$ T cell counts in the blood, but the $CD8^+$ T cells still responded to anti-CD47 treatment by significantly expanding (Figure 2C). Although the macrophage-depleted mice controlled plasma viremia very poorly, anti-CD47 treatment still resulted in a significant drop in viremia (Figure 2D). Thus, $CD8^+$ T cells could still expand in response to CD47 blockade and produce reductions in viremia. These results indicated that, although macrophages were important in the $CD8^+$ T cell responses and virus control, APCs other than macrophages were also stimulating the $CD8^+$ T cell responses. Since anti-CD47 also activated DCs, which are known to be important APCs for $CD8^+$ T cell responses, we tested mice carrying a transgenic diphtheria toxin (DT) receptor driven by the CD11c promoter such that delivery of DT depleted the DC population. Of note, a lower dose of LCMV was used in these experiments as the DT-treated mice could not tolerate high dose infection. Compared to non-depleted mice, DC-depleted mice had dramatically reduced $CD8^+$ T cell responses to LCMV infections and anti-CD47 treatment failed to elicit any significant $CD8^+$

T cell responses (Figure 2E). Furthermore, the DC-depleted mice had very high viremia, and no significant effect from anti-CD47 was observed (Figure 2F). These results indicated that the effects of CD47 blockade on $CD8^+$ T cells were mediated through DCs, likely by enhancing APC activity. To directly test whether CD47 blockade stimulated the APC function of DCs, *in vitro* cultures of peptide-loaded DCs were incubated for 24 h either with or without anti-CD47 antibody. The media was then removed and LCMV-specific $CD8^+$ T cells were added to the culture to test for stimulation. As expected, LCMV peptide-loaded DCs stimulated the $CD8^+$ T cells to divide (Figure 2G) and produce IFN-γ (Figure 2H). However, stimulation of the DCs with anti-CD47 prior to co-culture with $CD8^+$ T cells resulted in even greater proliferation (Ki-67 expression) and IFN-γ production by the $CD8^+$ T cells (Figures 2G and 2H). Thus, even in optimized *in vitro* stimulation conditions, CD47 blockade provided the DCs with additional capacity to stimulate $CD8^+$ T cells. Consistent with the results from the DC depletion experiments, these data further indicate that CD47 expression on DCs is important for the efficacy of CD47 blockade therapy.

SIRPα Expression on $CD8^+$ T Cells Not Required for CD47 Blockade Effects

The recent discovery that cytolytic $CD8^+$ T cell effectors express the CD47 receptor, SIRPα (Myers et al., 2019), suggested that CD47 blockade could have direct effects on $CD8^+$ T cell signaling. To investigate the role of SIRPα on $CD8^+$ T cells during immunotherapy, adoptive transfers of $CD8^+$ T cells from either wild-type (WT) mice or mice with genetic inactivation of the *SIRPa* gene (SIRPα knockout [KO]) were carried out using recipient mice that were genetically deficient in T cells due to targeted deletion of the alpha and beta T cell receptors (Mombaerts et al., 1992). The day after adoptive transfer of 2.5 million cells, the mice were infected with LCMV. Anti-CD47 therapy was carried out from 2 dpi until 6 dpi, and the mice were euthanized for evaluation at 10 and 13 dpi. SIRPα expression on $CD8^+$ T cells from LCMV-infected WT donor mice was evident at 13 dpi, whereas the donor cells from SIRPα KO mice showed no expression before or after infection (Figure 3A). The only significant difference observed between WT and SIRPα KO $CD8^+$ T cells was that the $CD8^+$ T cells from SIRPα KO mice expanded slightly but significantly less well than their wild-type counterparts at 10 dpi in mock-treated controls (Figure 3B). However, in the anti-CD47-treated mice, no differences between the donor types was observed indicating that anti-CD47-induced $CD8^+$ T cell expansion was not dependent on SIRPα expression on the $CD8^+$ T cells. The SIRPα KO $CD8^+$ T cells produced equivalent proportions of LCMV-specific tetramer$^+$ subpopulations (Figure 3C), $CD107a^+$ subpopulations (Figure 3D), and IFN-γ-producing subpopulations (Figure 3E). Mice receiving adoptive transfers of either WT or SIRPα KO $CD8^+$ T cells responded equally well to anti-CD47 therapy in better control of plasma viremia at 10 dpi (Figure 1F) and kidney virus at 13 dpi (Figure 3G).

CD47 Blockade during HIV-1 Infection of Humanized Mice

The finding that CD47 blockade led to reduced viral loads and enhanced innate and adaptive immune responses in LCMV infections in mice prompted us to further examine the applicability of this immunotherapeutic approach against viral infections. We tested anti-CD47 in a SCID-hu Thy/Liv mouse model of HIV-1. Humanized mice were generated by co-implantation of human fetal thymus and liver tissue beneath the kidney capsule of

recipient SCID mice as described (Namikawa et al., 1990; McCune et al., 1988). Humanized mouse models, such as the SCID-hu Thy/Liv model, are the only non-human animals that can be infected by pathogenic HIV, and the SCID-hu Thy/Liv model has been optimized and standardized for the preclinical evaluation of therapeutic drugs against HIV-1 (Stoddart et al., 2007). In the absence of therapy, HIV-1 infection of such mice generally leads to progressive loss of CD4-positive and CD4/CD8-double-positive cells in the thymic implant over the first month of infection (Bonyhadi et al., 1993; Stoddart et al., 2007). Immunotherapy with anti-CD47 was tested against an established infection, 6 weeks post-inoculation with the HIV-1 R5 strain, JR-CSF. Two cohorts of mice reconstituted with tissue from separate donors were tested. Both cohorts of mice were equivalently reconstituted as demonstrated by the total cell yields from uninfected control mice at the 9 week post-inoculation time point (Table 1). The mice were treated three times a week for 3 weeks with anti-CD47 or a control antibody. In the first cohort, tested mice treated with anti-CD47 had a small but statistically significant reduction in HIV-1 p24 compared to untreated mice (Table 1, top). Furthermore, the treated mice demonstrated protection from HIV-1-induced $CD4^+$ thymocyte depletion as they also had a small but statistically significant increase in CD4/CD8 ratios compared to untreated or control antibody-treated mice (Table 1). Of note, $CD4^+$ T cell depletion in the controls of this cohort was not as severe (47%–49% live thymocytes) as normally observed (Stoddart et al., 2007), suggesting that there was better inherent virus control than usual. A second cohort was tested that had more severe depletion levels (17% live thymocytes; Table 1, bottom) and in which no effect from anti-CD47 therapy was observed. These results suggested that the efficacy of CD47 blockade could be dependent on host factors and clearly more research in this area is warranted. Note, however: while these experiments were in progress, a Presidential Executive Order banned government scientists (including K.J.H.) from using human fetal tissue in research and canceled the funding for a contract (awarded to University of California, San Francisco [UCSF]) to test HIV therapeutics in humanized mice. Without a lifting of the ban, further experiments cannot go forward.

DISCUSSION

To date, a few studies addressing the role of CD47 in infectious diseases have been done comparing *Cd47*$^{-/-}$ mice with their wild-type counterparts, and the results vary depending on the infectious agent. In experimental infections with *Plasmodium* species, *Cd47*$^{-/-}$ mice had reduced parasitemia and enhanced survival compared to WT mice, which was attributed to enhanced phagocytosis of infected red blood cells (RBCs) (Ayi et al., 2016). Antibodies against SIRPα to block interactions with CD47 also enhanced survival in that study. Depending on the *Plasmodium* species, CD47 expression levels (for example on young versus old RBCs) can strongly regulate both parasite invasion of RBCs and phagocytic uptake by macrophages (Ayi et al., 2016; Banerjee et al., 2015). Additionally, in bacterial infection, deficiency of CD47 protects mice from LPS-induced acute lung injury and *E. coli* pneumonia (Su et al., 2008). An influenza vaccine study in *Cd47*$^{-/-}$ mice showed that they responded to vaccination with increased titers of virus-specific antibodies and were better protected than WT mice (Lee et al., 2016). In contrast to the studies showing better protection from infection in CD47-deficient mice, studies have also shown that CD47 may

play protective roles. For example, *Cd47*$^{-/-}$ mice showed increased morbidity and mortality during *Candida albicans* infection, with more widely disseminated infection along with elevated neutrophil, macrophage and CD4^{+} T cell infiltrates, and increased inflammatory cytokine levels, indicating poorly controlled pro-inflammatory responses (Navarathna et al., 2015). *Cd47*$^{-/-}$ mice have also been shown to have decreased levels of NK cells in their bone marrow and decreased NK responses to and control of chronic clone-13 LCMV infections (Nath et al., 2018).

A major drawback in interpreting results from studies on mice with genetic inactivation of CD47 is that lack of protein expression can exert dramatic impacts on development and differentiation as in the case of the diminished numbers of NK cells in the bone marrow of naive mice noted above. Lifelong absence of the CD47 “don’t-eat-me molecule” could allow emergence of cells induced to express or overexpress other “don’t-eat-me” molecules such as PDL1 (Gordon et al., 2017) or MHC class I β2-microglobulin (Barkal et al., 2018). It has also been shown that macrophages developing in *Cd47*$^{-/-}$ mice are tolerant to xenografts and their macrophages are not fully functional (Lavender et al., 2013). To study the role of CD47 at the time of an infection in mice that had matured with wild-type CD47 expression, we used a blocking monoclonal antibody following infection with LCMV. We observed that CD47 blockade significantly enhanced not only innate immune responses, as indicated by increased activation of macrophages (Figure 1D), but also enhanced the activation of DCs to induce better expansion of T cells *in vitro* (Figures 2G and 2H) and *in vivo* (Figures 1F–1I, 2E, 3C, and 3D). These results indicate that CD47 acts as a checkpoint molecule that not only keeps innate immune responses in check but also has downstream effects on the activation of adaptive immune responses. Our depletion experiments showed roles for both macrophages and DCs in the expansion of CD8^{+} T cells in response to LCMV infection, with DC depletions showing a much more profound effect on CD8+ T cell expansion, infection levels, and the ability to respond to anti-CD47 therapy (Figure 2). One caveat that should be noted is that certain macrophage subpopulations of the alveolar, lamina propria, metallophillic, and marginal zone express CD11c and are depleted by DT in CD11c-DTR^{tg} mice. Furthermore, some promiscuous expression of DTR occurs in CD11c-DTR^{tg} mice that can result in some depletion of non-DCs (Roberts et al., 2015). That said, those macrophages would likely have been depleted by the chlodronate treatments, which had much less effect on CD8^{+} T cells than the DT treatments.

If CD47 blockade was disrupting inhibitory interactions directly with the SIRPα receptor on CD8^{+} T cells, one would expect that CD8^{+} T cells from SIRPα knockout mice to be unresponsive to blockade. However, in adoptive transfer experiments, T cells from SIRPα knockout mice responded equivalently to WT T cells (Figure 3). This result indicates that the activating effects of CD47 blockade were not acting directly through SIRPα on the T cells, but rather, indirectly. This finding is consistent with our results indicating that the effect of CD47 blockade on CD8^{+} T cells was mediated via the better activation and APC function of DCs (Figure 2). Previously, it was shown that SIRPα expression on CD8^{+} T cells marked the functional effectors and that cytotoxic T lymphocyte (CTL) targets lacking CD47 expression were not killed as well by CD8^{+} CTLs (Myers et al., 2019). This result suggested that interactions between CD47 on target cells and SIRPα on CD8^{+} T cells were involved in, albeit not essential for cytolytic killing. While the current study did not directly

assess CTL killing, we found no evidence for an essential role for SIRPα expression on $CD8^+$ T cells in the resolution of LCMV infection. However, it was observed that the initial response of $SIRP\alpha^{+/+}$ $CD8^+$ T cells to infection was slightly, but significantly more robust than the response of $SIRP\alpha^{-/-}$ $CD8^+$ T cells (Figure 3B). Taken together, evidence from this *in vivo* acute infection in which $CD8^+$ T cells were critical for virus control (Figures 2A and 2D), indicated that SIRPα expression on $CD8^+$ T cells was expendable.

As an innate checkpoint inhibitor, anti-CD47 is unique in its ability to activate innate immune cells, and in doing so enhance downstream adaptive responses. More importantly, because CD47 is a host marker of self rather than a tumor or pathogen-specific cellular marker, the utility of CD47 blockade is not limited to a specific disease. There are currently several clinical trials evaluating the safety and efficacy of CD47 blockade in cancer patients (Advani et al., 2018), and our results demonstrate that this therapeutic approach may also be effective in human viral infections. Although preliminary, our results from one cohort of HIV-1-infected humanized (SCID-hu Thy/Liv) mice are consistent with the possibility that anti-CD47 can reduce viral loads and provide protection from $CD4^+$ T cell depletion, which we interpret as indicating that infected, and perhaps persistently infected, cells of as-yet-unknown phenotype have induced CD47 to protect them from phagocytosis. It is currently unclear why the two cohorts responded so differently to anti-CD47 treatment. Since HIV patients have been well documented to vary in susceptibility to HIV infection due to genetic resistance factors (Lama and Planelles, 2007), donor tissue susceptibility or resistance to infection may be one possible explanation for treatment differences. Anti-CD47 treatment was only efficacious in the cohort where HIV infection had a reduced effect on thymocyte depletion, suggesting that there may be an infection level threshold beyond which anti-CD47-mediated immune enhancement cannot be effective. Given the difficulty in eliciting immune-mediated reductions in established HIV infections, further investigation is certainly warranted should this model once again become available for testing. Other applications for CD47 blockade include non-resolving acute infections or persistent infections associated with Epstein-Barr virus, shingles, HPV, hepatitis B, and herpes simplex virus 2. In fact, the non-specific nature of the mechanism of action involved in CD47 blockade suggests that a wide range of pathogens, not just viruses, could be amenable to therapy.

STAR★METHODS

LEAD CONTACT AND MATERIALS AVAILABILITY

Further information and requests for resources and reagents should be directed to and will be fulfilled by the Lead Contact: Khasenkrug@nih.gov. This study did not generate new unique reagents.

EXPERIMENTAL MODEL AND SUBJECT DETAILS

Mice used in LCMV studies—Inbred C57BL/6J (WT) (RRID:IMSR_JAX:000664), and B6.129P2-Tcrb^{tm1Mom}/J (*TCRb*$^{-/-}$) (RRID:IMSR_JAX:002118) mice were purchased from Jackson Laboratory. P14 mice expressing the LCMV-GP33-41-specific TCR as a transgene were originally obtained from Prof. Tak W. Mak (The Campbell Family Cancer Research Institute and University Health Network, Toronto, Canada). P14 mice were maintained on

CD45.1 background and were used for $CD8^+$ T cell transfer and co-culture experiments (P14.CD45.1). The CD11c-DTR^{tg} mice were maintained on C57BL/6J background and experiments were performed at Prof. Phillip Lang's lab (Heinrich-Heine-University, Dusseldorf). B6.129P2-$Sirpa^{tm1Nog}$/Rbrc (SIRPα KO) (RRID:IMDR_RBRC01544) mice All experiments were performed using female mice, greater than 8 weeks of age, housed in ventilated cages and the health status of the mice was checked daily. Animal experiments were done with the authorization of Veterinäramt Nordrhein-Westfalen (Düsseldorf, Germany) and in accordance with the German law for animal protection.

***In vitro* CD8 activation with BMDCs—**Bone marrow-derived dendritic cells (BMDCs) were derived from bone marrow harvested from the tibiae and femurs of 8 week old female C57BL/6J mice. The cell suspensions were lysed of erythrocytes with ACK lysis buffer, washed, and cultured in 20ml VLE-DMEM media (FG1445; merckmillipore) supplemented with 5% culture supernatants containing murine GM-CSF (prepared in house from X63-GM-CSF cell line culture), 10% heat inactivated fetal bovine serum (10270; GIBCO), 1% penicillin, streptomycin and L-Glutamine solution (G6784 Sigma), and 0.1% 50mM beta mercaptoethanol (D4551, Sigma) to constitute a complete media (CM). The bone marrow cells were incubated at 37°C in a humidified atmosphere with 5% CO2 and fed another 20ml CM on day 3. On day five or six, the BMDCs were harvested for seeding in 24 well plates at 1×10^5/well with 10 μg/ml anti-CD47 or isotype control antibody for 24 hours. The media containing the antibody was removed and fresh media was added containing 5×10^5 naive CD8 T cells sorted from P14.CD45.1 mice, and 1 μg/ml of LCMV-gp33 or VSV-P52 control peptide. The co-cultures were analyzed after 3 days. The CD8 T cells were isolated from splenocytes of LCMV-specific transgenic P14.CD45.1 mice using $CD8^+$ T cell isolation kit (130-104-075, Miltenyi Biotec) and $CD8^+$ T cell were obtained using manufacturer's instructions.

SCID-hu Thy/Liv Mice—All SCID-hu Thy/Liv experiments were performed at UCSF, and animal protocols were approved by the UCSF Institutional Animal Care and Use Committee. SCID-hu Thy/Liv mice were generated by implanting 6- or 7-week old male C.B-17 SCID mice (RRID:IMSR_TAC:cb17sc) with 1 mm^3 pieces of fetal thymus and liver beneath the kidney capsule as previously described (Rabin et al., 1996; Stoddart et al., 2007). Each cohort was transplanted with tissue from a different donor (Table 1). At 19 or 26 weeks post-transplant (as indicated in Table 1), stock virus (1,000 $TCID_{50}$) or RPMI medium was injected directly into the surgically exposed Thy/Liv organ of anesthetized mice. Six-weeks post-inoculation, antibodies were diluted to 1.5 mg/mL in sterile Dulbecco's phosphate-buffered saline (PBS), and mice were treated with 300 μg anti-CD47 antibody, 5F9-hIgG4 (Lonza) or control antibody (Human IgG4 from Eureka Therapeutics Cat# ET904) three times a week, for three weeks. At that time the Thy/Liv implants were isolated from euthanized mice and dispersed through a sterile nylon mesh bag submerged in FASC buffer (PBS^+ 2% fetal bovine serum (FBS) to make single-cell suspensions for downstream analysis.

METHOD DETAILS

LCMV studies

CD47 blockade: The CD47 blockade was done via daily intraperitoneal injections of 100 μg of anti-CD47 (Clone 410 Cat#: BE0283) or isotype (rat IgG2a isotype) (Bio X Cell) from day 2 to day 6 post-infection.

Virus and plaque assays: The LCMV-WE virus stock (originally obtained from Prof. F. Lehmann-Grube, Heinrich Pette Institute, Hamburg, Germany) (Lehmann-Grube, 1971) was propagated on L929 cells. LCMV viral titers were detected by plaque-forming assays on MC57 fibroblasts (obtained from by the Ontario Cancer Institute, Canada) cultured at 37°C in Dulbecco's modified Eagle medium (DMEM) containing 2% fetal calf serum (FCS) and 1% penicillin/streptomycin. Organs were smashed and plasma was diluted in DMEM containing 2% FCS, titrated 1:3 over 12 steps, and incubated on MC57 cells. After 4 hours of incubation at 37°C, overlay methylcellulose was added and the cells were incubated for 48 hours followed by staining of LCMV plaques using an anti-LCMV-NP antibody (clone VL4).

***In vivo* cell depletions:** Macrophages were depleted with an intravenous injection of 300 ul/mouse of clodronate liposomes or no clodronate liposome controls at day −3 prior to infection. Both the clodronate liposomes and liposome controls were purchased at Liposoma B.V., Amsterdam, Netherlands. In the $CD8^+$ T cell depletion experiments, 500 μg of anti-CD8 depleting antibody (clone 2.43 cat no. BE0061 Bio X Cell) was injected i.p at days −3 and day 1 relative to infection. $CD4^+$ T cells were depleted in the same manner using 500 μg/mouse anti-CD4 (clone GK1.5 cat no. BE0003-1 Bio X Cell). The $CD11c^+$ DCs were depleted using CD11c-DTR^{tg} mice treated i.p with diphtheria toxin (Cat no. MFCD00163490, Sigma Aldrich) at 100ng/mouse at day −2 prior to infection. Cell subset depletions were confirmed by FACS analysis to be greater than 90% for all of the respective cells.

Flow cytometry: Tetramers were provided by the Tetramer Facility of the National Institutes of Health (NIH; Bethesda, MD, USA). Cells were stained with allophycocyanin-labeled GP33 (GP33/H-2Db) and NP396 MHC class I tetramers for 15 min at 37°C and then with indicated antibodies for 30 min at 4°C. For blood samples, erythrocytes were lysed with 1 mL BD lysing solution (BD Biosciences), washed once with fluorescence-activated cell sorting (FACS) buffer, and analyzed by flow cytometry. Absolute numbers of cells were calculated based on results from fluorescent calibrating beads (BD Biosciences). Surface antibodies: CD8a (53–6.7), CD19 (eBio1D3 (1D3)), NK1.1 (PK136), CD3e CD4 (GK1.5), CD11c (N418), MHC class II (M5/114.15.2), F4/80 (BM8), CD107a (LAMP-1) and CD80 (16–10A1), were purchased from Thermo-fisher. Antibodies CD11b (M/70), CD44 (IM7) and CD86 (GL1) purchased from BD Biosciences. Stained cells were analyzed on a FACS Fortessa flow cytometer (BD Biosciences), and data were analyzed with the FlowJo software (FlowJo LLC, Ashland, OR, USA).

Intracellular cytokine staining: Spleens were homogenized, lysed with Ammonium-Chloride-Potassium (ACK) and cells were re-stimulated at 37°C with LCMV-GP33-specific

peptide (PolyPeptide Laboratories, Strasbourg, France) for 6 h. Brefeldin A (BFA) was added for the last 5 hours. Cells were then stained for 30 minutes with surface markers, fixed with 2% formaldehyde solution in PBS for 10 min, permeabilized with 1% saponin solution, and then stained with anti-IFNγ (XMG 1.1, eBioscience) or TNF (MP6-XT22, eBioscience) antibodies for 30 minutes at 4°C.

Adoptive Transfer of CD8$^+$ T cells: CD8$^+$ T cells were bead purified from splenocytes of WT or SIRPα KO mice using CD8$^+$ T cell isolation kit (130-104-075, Miltenyi Biotec) and CD8$^+$ T cells were obtained using procedure according to the manufacturer. 2.5×10^6 naive CD8 T cells from WT or SIRPα KO mice were transferred intravenously to *TCRb*$^{-/-}$ mice at day −1. The recipient *TCRb*$^{-/-}$ mice were then infected i.v with LCMV-WE at a dose of 1×10^4 PFU and mice were then treated with 100 μg/mouse of anti-CD47 or isotype at day 2 to day 6 post infection.

HIV Studies

HIV-1 Virus: HIV molecular clone pYK-JRCSF (R5) from Dr. Irvin SY Chen and Dr. Yoshio Koyanagi (Cann et al., 1990; Haltiner et al., 1985; Koyanagi et al., 1987) was obtained through the NIH AIDS Research and Reference Reagent Program, Division of AIDS, NIAID, NIH. Working stocks were prepared in HEK293T cells by lipofectamine 2000 transfection, and virus was titrated in phytohemagglutinin (PHA)-activated peripheral blood mononuclear cells (PBMCs) to determine the $TCID_{50}$ (50% tissue culture infectious dose) by limiting dilution and HIV-1 p24 detection at day 7 by ELISA.

p24 ELISA: To quantify HIV-1 antigen p24, 2.5×10^6 cells from the Thy/Liv single cell suspension were lysed overnight at 4°C in lysing buffer (containing 1% Triton X-100, 0.5% deoxycholate, 5 mM EDTA, 25 mM Tris HCl, 250 mM NaCl, and 1% aprotinin) and stored at −20°C. Cell lysates were transferred to HIV-1 p24 coated plates for quantitative ELISA (PerkinElmer Life Sciences), a standard curve was generated from supplied standards, and results were calculated as pg/10^6 cells.

Branched DNA assay: 5×10^6 cells from the Thy/Liv single cell suspension were stored as dry pellets at −80°C. Prior to bDNA assay cells were lysed mechanically in sterile disposable pestles and motor grinder (Kontes) in M guanidine HCl with 0.5% sodium N-lauroylsarcosine. RNA was then extracted with 500 uL 100% ethanol and pelleted at 12,000 × g for 20 min at 4°C. The RNA pellet was washed with 500 uL 70% ethanol and digested using supplied reagents according to manufacturer instructions of the VERSANT HIV-1 RNA 3.0 Assay (Siemens Healthcare Diagnostics). HIV-1 RNA is expressed as copies/10^6 cells, and $\log_{10}$ values were used to calculate geometric means.

Flow Cytometry Analysis of Thymocytes: Flow cytometry was used at the 6 weeks post infection time point to confirm implant quality. 1×10^6 cell were used to analysis. Total Thy/Liv cellularity was then determined by cell count with a Coulter counter. Thymocyte subpopulations of all mice were determined by flow cytometric analysis of 1×10^6 cells from Thy/Liv single cell suspensions. Cells were stained in FACS buffer with antibodies for CD3, CD4, and CD8 and to quantify thymocyte subpopulations.

QUANTIFICATION AND STATISTICAL ANALYSIS

Student's t tests were used to detect statistically significant differences between 2 groups. Significant differences between more than two groups were detected by one-way analysis of variance (ANOVA) with multiple comparisons post hoc tests, or by Mann-Whitney U test as indicated in the figure and table legends. The level of statistical significance was set at $p = 0.05$. Statistical comparisons were performed using GraphPad Prism version 7.0d for Mac, GraphPad Software, La Jolla California USA.

DATA AND CODE AVAILABILITY

This study did not generate or analyze datasets/codes.

Supplementary Material

Refer to Web version on PubMed Central for supplementary material.

ACKNOWLEDGMENTS

This research was funded by a Deutsche Forschungsgemeinschaft (DFG) grant through the Research Training Group (RTG) 1949, University of Duisburg-Essen (L.B.C. and K.S.L.); the Deutsche Forschungsgemeinschaft (DFG) grants LA1419/7-1, LA1419/10-1, the collaborative research centre CCR974 and the Research Training Groups RTG2098, Germany (L.B.C. and K.S.L.), the Intramural Research Program of the National Institute of Allergy and Infectious Diseases, National Institutes of Health, USA (K.J.H.); Virginia and D.K. Ludwig Fund for Cancer Research; the Robert J. Kleberg, Jr. and Helen C. Kleberg Foundation, and the Virginia and Daniel Ludwig Cancer Foundation, USA. M.C.T. was supported by Stanford Immunology Training Grant 5T32AI007290, the Bay Area Lyme Foundation and NIH NRSA Grant 1 F32 AI124558-01, USA. L.B.T.D. was supported by the Stanford Diversifying Academia, Recruiting Excellence fellowship. National Institutes of Health (NIH, USA) Tetramer Core Facility provided the tetramers. This work was supported in part by federal funds from NIAID, NIH, USA under Contract HHSN266200700002C/N01-AI-70002. The funders had no role in study design, data collection, and analysis, decision to publish, or preparation of the manuscript.

REFERENCES

Advani R, Flinn I, Popplewell L, Forero A, Bartlett NL, Ghosh N, Kline J, Roschewski M, LaCasce A, Collins GP, et al. (2018). CD47 blockade by Hu5F9-G4 and rituximab in non-Hodgkin's lymphoma. N. Engl. J. Med 379, 1711–1721. [PubMed: 30380386]

Ayi K, Lu Z, Serghides L, Ho JM, Finney C, Wang JCY, Liles WC, and Kain KC (2016). CD47-SIRPα interactions regulate macrophage uptake of *Plasmodium falciparum*-infected erythrocytes and clearance of malaria in vivo. Infect. Immun 84, 2002–2011. [PubMed: 27091932]

Banerjee R, Khandelwal S, Kozakai Y, Sahu B, and Kumar S (2015). CD47 regulates the phagocytic clearance and replication of the *Plasmodium yoelii* malaria parasite. Proc. Natl. Acad. Sci. USA 112, 3062–3067. [PubMed: 25713361]

Barclay AN, and Van den Berg TK (2014). The interaction between signal regulatory protein alpha (SIRPα) and CD47: structure, function, and therapeutic target. Annu. Rev. Immunol 32, 25–50. [PubMed: 24215318]

Barkal AA, Weiskopf K, Kao KS, Gordon SR, Rosental B, Yiu YY, George BM, Markovic M, Ring NG, Tsai JM, et al. (2018). Engagement of MHC class I by the inhibitory receptor LILRB1 suppresses macrophages and is a target of cancer immunotherapy. Nat. Immunol 19, 76–84. [PubMed: 29180808]

Betancur PA, Abraham BJ, Yiu YY, Willingham SB, Khameneh F, Zarnegar M, Kuo AH, McKenna K, Kojima Y, Leeper NJ, et al. (2017). A CD47-associated super-enhancer links pro-inflammatory signalling to CD47 upregulation in breast cancer. Nat. Commun 8, 14802. [PubMed: 28378740]

Bian Z, Shi L, Guo YL, Lv Z, Tang C, Niu S, Tremblay A, Venkataramani M, Culpepper C, Li L, et al. (2016). Cd47-Sirpα interaction and IL-10 constrain inflammation-induced macrophage

phagocytosis of healthy self-cells. Proc. Natl. Acad. Sci. USA 113, E5434–E5443. [PubMed: 27578867]

Bonyhadi ML, Rabin L, Salimi S, Brown DA, Kosek J, McCune JM, and Kaneshima H (1993). HIV induces thymus depletion in vivo. Nature 363, 728–732. [PubMed: 8100043]

Cameron CM, Barrett JW, Liu L, Lucas AR, and McFadden G (2005a). Myxoma virus M141R expresses a viral CD200 (vOX-2) that is responsible for down-regulation of macrophage and T-cell activation in vivo. J. Virol 79, 6052–6067. [PubMed: 15857991]

Cameron CM, Barrett JW, Mann M, Lucas A, and McFadden G (2005b). Myxoma virus M128L is expressed as a cell surface CD47-like virulence factor that contributes to the downregulation of macrophage activation in vivo. Virology 337, 55–67. [PubMed: 15914220]

Campbell IG, Freemont PS, Foulkes W, and Trowsdale J (1992). An ovarian tumor marker with homology to vaccinia virus contains an IgV-like region and multiple transmembrane domains. Cancer Res. 52, 5416–5420. [PubMed: 1394148]

Cann AJ, Zack JA, Go AS, Arrigo SJ, Koyanagi Y, Green PL, Koyanagi Y, Pang S, and Chen IS (1990). Human immunodeficiency virus type 1 T-cell tropism is determined by events prior to provirus formation. J. Virol 64, 4735–4742. [PubMed: 2398528]

Chao MP, Alizadeh AA, Tang C, Myklebust JH, Varghese B, Gill S, Jan M, Cha AC, Chan CK, Tan BT, et al. (2010). Anti-CD47 antibody synergizes with rituximab to promote phagocytosis and eradicate non-Hodgkin lymphoma. Cell 142, 699–713. [PubMed: 20813259]

Chao MP, Alizadeh AA, Tang C, Jan M, Weissman-Tsukamoto R, Zhao F, Park CY, Weissman IL, and Majeti R (2011). Therapeutic antibody targeting of CD47 eliminates human acute lymphoblastic leukemia. Cancer Res. 71, 1374–1384. [PubMed: 21177380]

Ciurea A, Klenerman P, Hunziker L, Horvath E, Odermatt B, Ochsenbein AF, Hengartner H, and Zinkernagel RM (1999). Persistence of lymphocytic choriomeningitis virus at very low levels in immune mice. Proc. Natl. Acad. Sci. USA 96, 11964–11969. [PubMed: 10518559]

Fung-Leung WP, Kündig TM, Zinkernagel RM, and Mak TW (1991). Immune response against lymphocytic choriomeningitis virus infection in mice without CD8 expression. J. Exp. Med 174, 1425–1429. [PubMed: 1683893]

Gao Q, Chen K, Gao L, Zheng Y, and Yang YG (2016). Thrombospondin-1 signaling through CD47 inhibits cell cycle progression and induces senescence in endothelial cells. Cell Death Dis. 7, e2368. [PubMed: 27607583]

Gordon SR, Maute RL, Dulken BW, Hutter G, George BM, McCracken MN, Gupta R, Tsai JM, Sinha R, Corey D, et al. (2017). PD-1 expression by tumour-associated macrophages inhibits phagocytosis and tumour immunity. Nature 545, 495–499. [PubMed: 28514441]

Gu S, Ni T, Wang J, Liu Y, Fan Q, Wang Y, Huang T, Chu Y, Sun X, and Wang Y (2018). CD47 blockade inhibits tumor progression through promoting phagocytosis of tumor cells by M2 polarized macrophages in endometrial cancer. J. Immunol. Res 2018, 6156757. [PubMed: 30525058]

Haltiner M, Kempe T, and Tjian R (1985). A novel strategy for constructing clustered point mutations. Nucleic Acids Res. 13, 1015–1025. [PubMed: 2987803]

Isenberg JS, Ridnour LA, Dimitry J, Frazier WA, Wink DA, and Roberts DD (2006). CD47 is necessary for inhibition of nitric oxide-stimulated vascular cell responses by thrombospondin-1. J. Biol. Chem 281, 26069–26080. [PubMed: 16835222]

Jaiswal S, Jamieson CH, Pang WW, Park CY, Chao MP, Majeti R, Traver D, van Rooijen N, and Weissman IL (2009). CD47 is upregulated on circulating hematopoietic stem cells and leukemia cells to avoid phagocytosis. Cell 138, 271–285. [PubMed: 19632178]

Koyanagi Y, Miles S, Mitsuyasu RT, Merrill JE, Vinters HV, and Chen IS (1987). Dual infection of the central nervous system by AIDS viruses with distinct cellular tropisms. Science 236, 819–822. [PubMed: 3646751]

Lama J, and Planelles V (2007). Host factors influencing susceptibility to HIV infection and AIDS progression. Retrovirology 4, 52. [PubMed: 17651505]

Lavender KJ, Pang WW, Messer RJ, Duley AK, Race B, Phillips K, Scott D, Peterson KE, Chan CK, Dittmer U, et al. (2013). BLT-humanized C57BL/6 Rag2$^{-/-}\gamma c^{-/-}$CD47$^{-/-}$ mice are resistant to

GVHD and develop B- and T-cell immunity to HIV infection. Blood 122, 4013–4020. [PubMed: 24021673]

Lee YT, Ko EJ, Lee Y, Lee YN, Bian Z, Liu Y, and Kang SM (2016). CD47 plays a role as a negative regulator in inducing protective immune responses to vaccination against influenza virus. J. Virol 90, 6746–6758. [PubMed: 27194758]

Lehmann-Grube F (1971). Lymphocytic Choriomeningitis Virus (Springer-Verlag).

Lindberg FP, Bullard DC, Caver TE, Gresham HD, Beaudet AL, and Brown EJ (1996). Decreased resistance to bacterial infection and granulocyte defects in IAP-deficient mice. Science 274, 795–798. [PubMed: 8864123]

Liu X, Pu Y, Cron K, Deng L, Kline J, Frazier WA, Xu H, Peng H, Fu YX, and Xu MM (2015). CD47 blockade triggers T cell-mediated destruction of immunogenic tumors. Nat. Med 21, 1209–1215. [PubMed: 26322579]

Liu X, Kwon H, Li Z, and Fu YX (2017). Is CD47 an innate immune checkpoint for tumor evasion? J. Hematol. Oncol 10, 12. [PubMed: 28077173]

Majeti R, Chao MP, Alizadeh AA, Pang WW, Jaiswal S, Gibbs KD Jr., van Rooijen N, and Weissman IL (2009). CD47 is an adverse prognostic factor and therapeutic antibody target on human acute myeloid leukemia stem cells. Cell 138, 286–299. [PubMed: 19632179]

McCune JM, Namikawa R, Kaneshima H, Shultz LD, Lieberman M, and Weissman IL (1988). The SCID-hu mouse: murine model for the analysis of human hematolymphoid differentiation and function. Science 241, 1632–1639. [PubMed: 2971269]

Mombaerts P, Clarke AR, Rudnicki MA, Iacomini J, Itohara S, Lafaille JJ, Wang L, Ichikawa Y, Jaenisch R, Hooper ML, et al. (1992). Mutations in T-cell antigen receptor genes alpha and beta block thymocyte development at different stages. Nature 360, 225–231. [PubMed: 1359428]

Moskophidis D, Battegay M, van den Broek M, Laine E, Hoffmann-Rohrer U, and Zinkernagel RM (1995). Role of virus and host variables in virus persistence or immunopathological disease caused by a non-cytolytic virus. J. Gen. Virol 76, 381–391. [PubMed: 7531218]

Myers LM, Tal MC, Torrez Dulgeroff LB, Carmody AB, Messer RJ, Gulati G, Yiu YY, Staron MM, Angel CL, Sinha R, et al. (2019). A functional subset of $CD8^+$ T cells during chronic exhaustion is defined by SIRPα expression. Nat. Commun 10, 794. [PubMed: 30770827]

Namikawa R, Weilbaecher KN, Kaneshima H, Yee EJ, and McCune JM (1990). Long-term human hematopoiesis in the SCID-hu mouse. J. Exp. Med 172, 1055–1063. [PubMed: 2212942]

Nath PR, Gangaplara A, Pal-Nath D, Mandal A, Maric D, Sipes JM, Cam M, Shevach EM, and Roberts DD (2018). CD47 expression in natural killer cells regulates homeostasis and modulates immune response to lymphocytic choriomeningitis virus. Front. Immunol 9, 2985. [PubMed: 30643501]

Navarathna DH, Stein EV, Lessey-Morillon EC, Nayak D, Martin-Manso G, and Roberts DD (2015). CD47 promotes protective innate and adaptive immunity in a mouse model of disseminated candidiasis. PLoS ONE 10, e0128220. [PubMed: 26010544]

Rabin L, Hincenbergs M, Moreno MB, Warren S, Linquist V, Datema R, Charpiot B, Seifert J, Kaneshima H, and McCune JM (1996). Use of standardized SCID-hu Thy/Liv mouse model for preclinical efficacy testing of anti-human immunodeficiency virus type 1 compounds. Antimicrob. Agents Che-mother 40, 755–762.

Roberts LM, Ledvina HE, Tuladhar S, Rana D, Steele SP, Sempowski GD, and Frelinger JA (2015). Depletion of alveolar macrophages in CD11c diphtheria toxin receptor mice produces an inflammatory response. Immun. Inflamm. Dis 3, 71–81. [PubMed: 26029367]

Schürch CM, Roelli MA, Forster S, Wasmer MH, Brühl F, Maire RS, Di Pancrazio S, Ruepp MD, Giger R, Perren A, et al. (2019). Targeting CD47 in anaplastic thyroid carcinoma enhances tumor phagocytosis by macrophages and is a promising therapeutic strategy. Thyroid 29, 979–992. [PubMed: 30938231]

Sick E, Jeanne A, Schneider C, Dedieu S, Takeda K, and Martiny L (2012). CD47 update: a multifaceted actor in the tumour microenvironment of potential therapeutic interest. Br. J. Pharmacol 167, 1415–1430. [PubMed: 22774848]

Stoddart CA, Bales CA, Bare JC, Chkhenkeli G, Galkina SA, Kinkade AN, Moreno ME, Rivera JM, Ronquillo RE, Sloan B, and Black PL (2007). Validation of the SCID-hu Thy/Liv mouse model with four classes of licensed antiretrovirals. PLoS ONE 2, e655. [PubMed: 17668043]

Su X, Johansen M, Looney MR, Brown EJ, and Matthay MA (2008). CD47 deficiency protects mice from lipopolysaccharide-induced acute lung injury and *Escherichia coli* pneumonia. J. Immunol 180, 6947–6953. [PubMed: 18453616]

Toledano N, Gur-Wahnon D, Ben-Yehuda A, and Rachmilewitz J (2013). Novel CD47: SIRPα dependent mechanism for the activation of STAT3 in antigen-presenting cell. PLoS ONE 8, e75595. [PubMed: 24073274]

Tseng D, Volkmer JP, Willingham SB, Contreras-Trujillo H, Fathman JW, Fernhoff NB, Seita J, Inlay MA, Weiskopf K, Miyanishi M, and Weissman IL (2013). Anti-CD47 antibody-mediated phagocytosis of cancer by macrophages primes an effective antitumor T-cell response. Proc. Natl. Acad. Sci. USA 110, 11103–11108. [PubMed: 23690610]

Vaeteewoottacharn K, Kariya R, Pothipan P, Fujikawa S, Pairojkul C, Waraasawapati S, Kuwahara K, Wongkham C, Wongkham S, and Okada S (2019). Attenuation of CD47-SIRPα signal in cholangiocarcinoma potentiates tumor-associated macrophage-mediated phagocytosis and suppresses intrahepatic metastasis. Transl. Oncol 12, 217–225. [PubMed: 30415063]

Weiskopf K, Jahchan NS, Schnorr PJ, Cristea S, Ring AM, Maute RL, Volkmer AK, Volkmer JP, Liu J, Lim JS, et al. (2016). CD47-blocking immunotherapies stimulate macrophage-mediated destruction of small-cell lung cancer. J. Clin. Invest 126, 2610–2620. [PubMed: 27294525]

Zapata JC, Pauza CD, Djavani MM, Rodas JD, Moshkoff D, Bryant J, Ateh E, Garcia C, Lukashevich IS, and Salvato MS (2011). Lymphocytic choriomeningitis virus (LCMV) infection of macaques: a model for Lassa fever. Antiviral Res. 92, 125–138. [PubMed: 21820469]

Highlights

- CD47 “don’t-eat-me” signals are upregulated on infected cells
- Antibody-mediated blockade of CD47 enhances APC function *in vivo*
- Therapeutic CD47 blockade enhances T cell responses and speeds LCMV clearance
- CD47 blockade works in a pathogen non-specific manner to enhance immunity

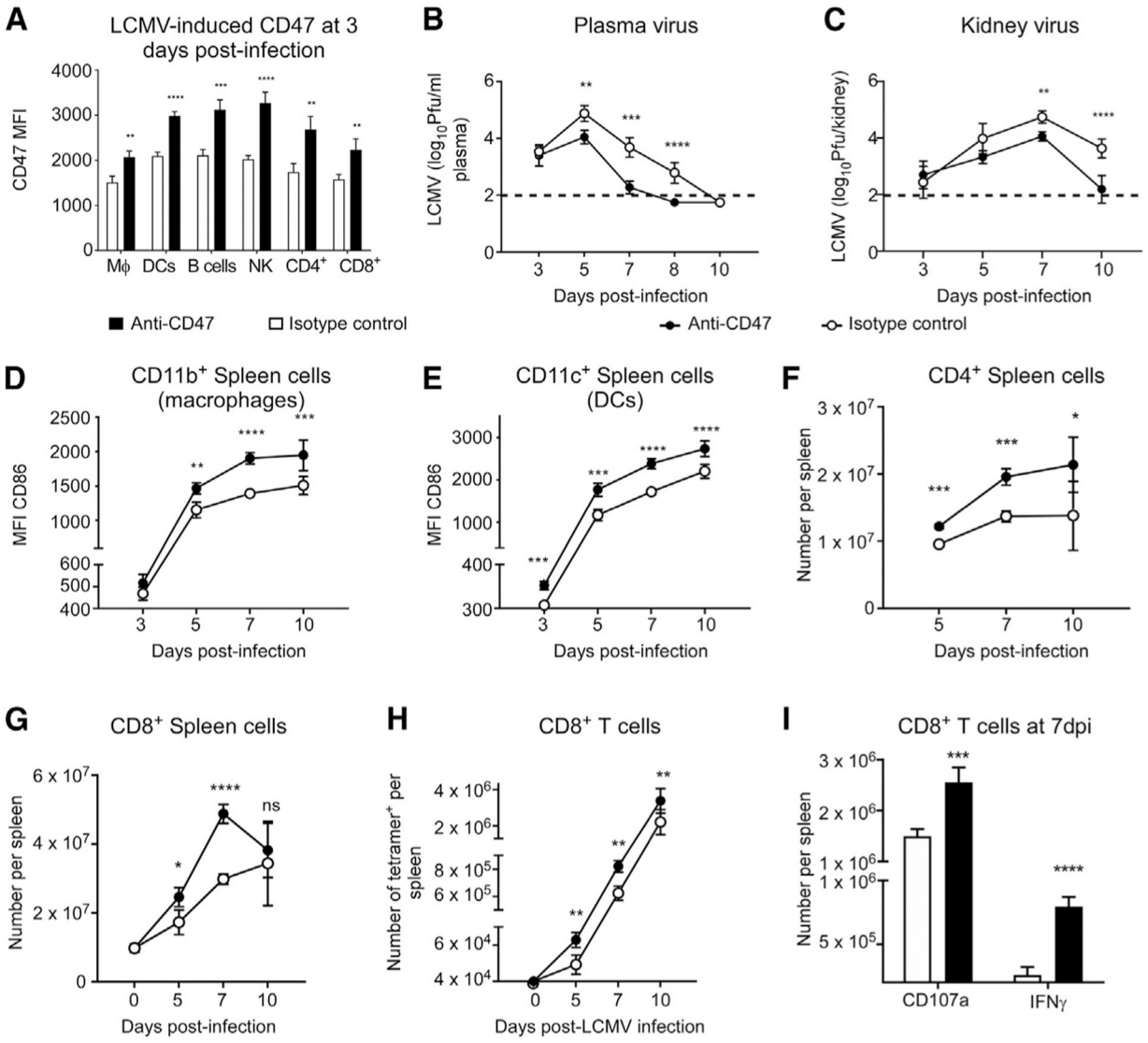

Figure 1. Effects of CD47 Blockade on LCMV Infection in Mice

(A) CD47 cell surface expression on splenic cell subsets was analyzed by flow cytometry at 3 days post-infection with LCMV-WE-infected C57BL/6 mice. The gating strategy for the spleen cell subsets is shown in Figure S1. n = 4 mice per group. (B–I) C57BL/6 mice infected with 2×10^6 PFU LCMV-WE were treated by intraperitoneal injection of 100 μg of anti-CD47 or isotype at days 2, 3, 4, 5, and 6 post-infection and analyzed on the indicated days post-infection for (B) plasma virus titers, (C) kidney virus titers, (D) CD86 expression on splenic macrophages, and (E) dendritic cells analyzed from anti-CD47-treated and control mice. Mice were also analyzed for (F) total number of $CD4^+$ and (G) $CD8^+$ T cells in the spleens of mice treated with anti-CD47 or isotype control antibody. Two-way ANOVA analysis showed a statistically significant difference in the kinetics for $CD4^+$ T cells ($p = 0.004$) and $CD8^+$ T cells ($p = 0.0002$). The $CD8^+$ T cells were further analyzed for the following: (H) total numbers of GP33-Tet^+ $CD8^+$ T cells at the indicated time points and (I) the numbers of $CD107a^+$ and IFN-γ^+ cells at 7 dpi, the peak of the $CD8^+$ T cell response.

Data shown are consistent with two independent experiments (n = 7) and are shown as mean ± SEM. Statistics comparing treated versus control mice were done by Student's t test: *p < 0.05, **p < 0.01, ***p < 0.001, and ****p < 0.0001.

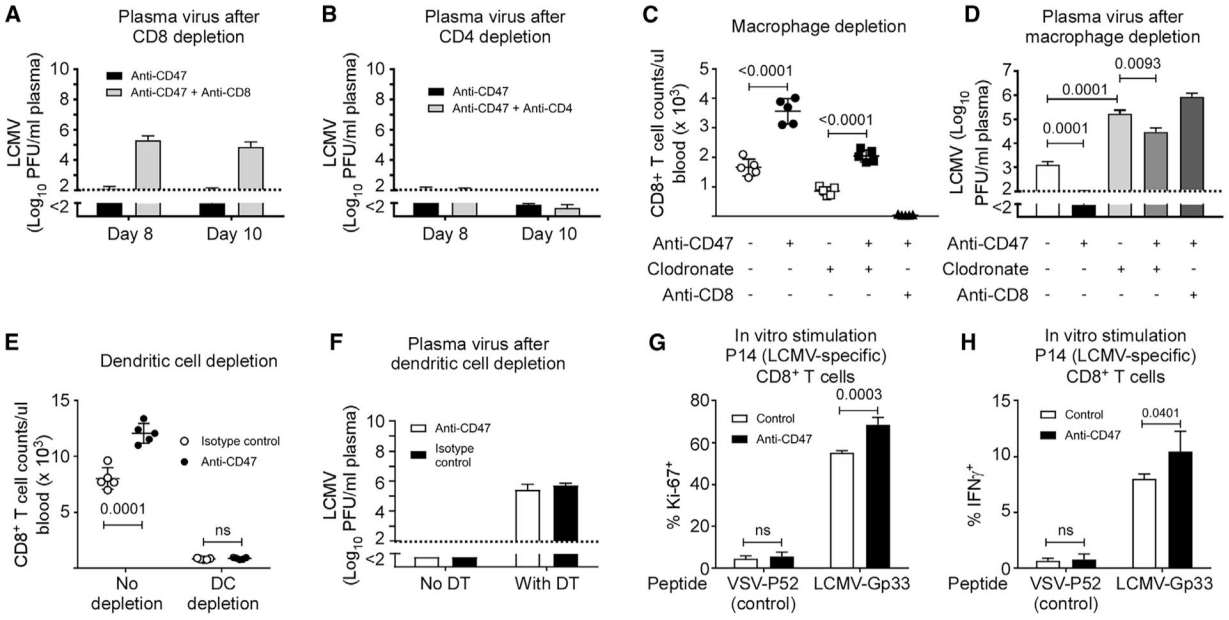

Figure 2. Involvement of Various Cell Subsets in the Mechanism of Protection by CD47 Blockade Therapy

(A and B) Plasma virus titers from C57BL/6 mice treated at day −1 and day 3 (relative to infection with 2×10^6 PFU LCMV-WE) by intraperitoneal injection of (A) 500 μg of anti-CD8 or isotype, (B) 500 μg of anti-CD4, and then treated by intraperitoneal injection of 100 μg of anti-CD47 at days 2, 3, 4, 5, and 6 post-infection. Mice were bled on days 8 and 10 for analysis (n = 4 mice/group).

(C and D) C57BL/6 mice were treated or not (as indicated) at day −3 (relative to infection with 2×10^6 PFU LCMV-WE) by intraperitoneal injection of 300 μL of chlodronate or liposome control, and 500 μg of anti-CD8 or isotype control antibody. Mice were then infected with 2×10^6 PFU LCMV-WE and treated (as indicated) intraperitoneally with 100 μg of anti-CD47 or isotype control antibody at days 2, 3, 4, 5, and 6 post-infection. (C) Total $CD8^+$ T cells count from blood at 8 dpi and (D) plasma virus titers at 8 dpi (n = 5 mice/group). Statistics for (C) were done by Student's t test and for (D) with a one-way ANOVA with Tukey's multiple-comparisons post-test. The p values are shown for comparisons of interest.

(E and F) $CD11c\text{-}DTR^{tg}$ mice (five mice/group) were injected i.p with 100 ng of diphtheria toxin or PBS/mouse at day −2 and then infected with 2×10^4 PFU of LCMV-WE. Mice were treated intraperitoneally with 100 μg of anti-CD47 or isotype control antibody as indicated at days 2, 3, 4, 5, and 6 post-infection. (E) Total number of $CD8^+$ T cells and (F) plasma virus titers from blood at 8 dpi. Statistics were done by Student's t tests. No statistically significant differences were observed in (F).

(G and H) *In vitro* stimulation of 5×10^5 naive $CD8^+$ T cells sorted from P14.CD45.1 (LCMV-specific TCR Tg) mice co-cultured with 1×10^5 wild-type bone marrow-derived DCs that were pretreated with 10 μg/mL anti-CD47 or isotype control and loaded with 1 μg/mL LCMV-gp33 or VSV-P52 control peptide antibody for 24 h. Co-cultures were analyzed after 72 h for percentages of (G) $Ki\text{-}67^+$ $CD8^+$ T cells and (H) $IFN\text{-}\gamma^+$ $CD8^+$ T cells. The dashed lines indicate the limit of detection for virus assays. Data shown are

consistent with at least two independent experiments and are shown as mean ± SEM (n = 4 mice/group). ns, not significant; Student's t tests were used to determine p values shown. The gating strategy for the spleen cell subsets is shown in Figure S1.

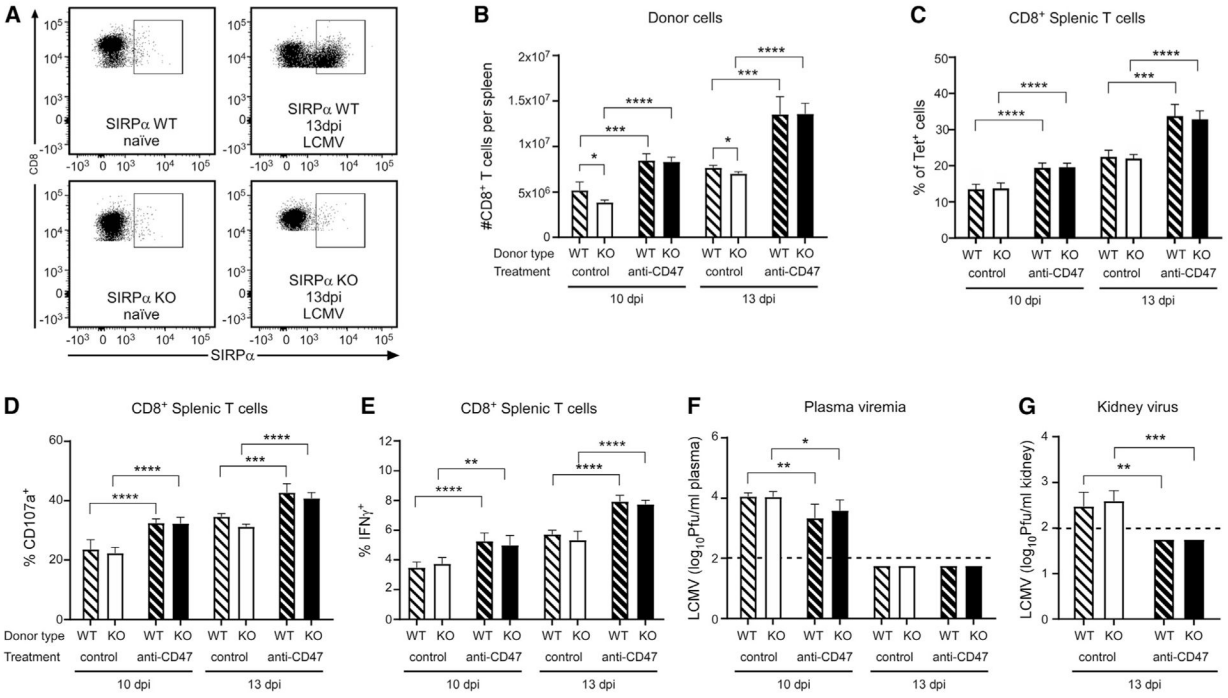

Figure 3. *In Vivo* Responses of *SIRPa*$^{+/+}$ or *SIRPa*$^{-/-}$ CD8$^+$ T Cells in LCMV-Infected Mice Treated with Anti-CD47

(A–G) Representative flow-cytometric plots of SIRPα expression on (A) CD8$^+$ T cells from spleens of naive WT (*SIRPa*$^{+/+}$) and SIRPα KO (*SIRPa*$^{-/-}$) C57BL/6 mice (left), and from the same strains infected with LCMV-WE at 13 dpi (right). (B–G) 2.5×10^6 naive CD8$^+$ T cells were sorted from splenocytes of WT or SIRPα KO mice (indicated as donor type) and were transferred intravenously into *TCRb*$^{-/-}$ mice at day −1. The recipient *TCRb*$^{-/-}$ mice were then infected i.v. with 1×10^4 PFU LCMV-WE i.v. and then treated daily with 100 μg/mouse of anti-CD47 or isotype control antibody from day 2 to day 6 post-infection. Mice were euthanized for analyses at 10 dpi (n = 5 mice/group) and 13 dpi (n = 4 mice/group). Cumulative results from flow-cytometric analysis of (B) total splenic CD8$^+$ T cells, (C) percentages of GP33-Tet$^+$ CD8$^+$ T cells, (D) percentages of CD107a$^+$ CD8$^+$ T cells, (E) percentages of IFN-γ-producing CD8$^+$ T cells as measured by intracellular cytokine flow cytometry, (F) plasma viremia analyzed at 10 and 13 dpi, and (G) kidney virus levels at 13 dpi. The dashed lines indicate the limit of detection for virus assays. Data shown are means ± SEM. Statistics were done by ordinary one-way ANOVA with Tukey's multiple-comparisons post-test: *$p < 0.05$, **$p < 0.01$, ***$p < 0.001$, and ****$p < 0.0001$. The gating strategy for the spleen cell subsets is shown in Figure S1.

Table 1.

Evaluation of Anti-CD47 Immunotherapy against Established HIV-1 Infection in SCID-hu Thy/Liv Mice

Group	Mice/ Group	Virus	Drug Dose	p24 (pg/10^6 Cells)	p24 (% of Control)	HIV-1 RNA (Log_{10} Copies/10^6 Cells)	FACS Analysis: Live Thymocytes (%)	FACS Analysis: $CD4^+CD8^+$ (%)	FACS Analysis: $CD4^+$ (%)	FACS Analysis: $CD8^+$ (%)	FACS Analysis: CD4/CD8 Ratio	Total Cell Yield (10^6)	Live Thymocyte Yield (10^6)
Mice Infected 26 Weeks Post-engraftment													
A[a]	7	JR-CSF	300 μg anti-CD47	47 ± 6.3*	29 ± 3.9	4.4 ± 0.17	44 ± 5.2	70 ± 7.5	18 ± 5.3	6.8 ± 1.8	2.6 ± 0.13*	110 ± 64	57 ± 36
B[a]	6	JR-CSF	300 μg control Ab	96 ± 14**	60 ± 8.9	4.5 ± 0.16	47 ± 3.6	84 ± 1.7**	7.7 ± 0.39**	4.1 ± 0.41	1.9 ± 0.11**	140 ± 32	63 ± 13
C	6	JR-CSF	untreated	160 ± 43	100 ±27	4.8 ± 0.16	49 ± 2.8	76 ± 4.6	9.3 ± 1.4	4.9 ± 0.53	1.8 ± 0.13	240 ± 72	120 ± 40
D	6	medium	–	negative	0.0 ± 0.0	negative	45 ± 6.8	78 ± 6.3	13 ± 4.4	4.3 ±1.0	2.7 ± 0.20	190 ± 49	99 ± 29
Mice Infected 19 Weeks Post-engraftment													
A[b]	10	JR-CSF	300 μg anti-CD47	580 ± 110***	180 ± 34	5.0 ± 0.23	13 ± 2.6	19 ± 7.5	17 ± 2.9	28 ± 3.9***	0.75 ± 0.21	11 ± 1.6	1.5 ± 0.3
B	10	JR-CSF	300 μg control Ab	380 ± 47	120 ± 15	5.4 ±0.18	17 ± 3.2	18 ± 5.6	16 ± 2.4	25 ± 3.6***	0.69 ± 0.13	12 ± 1.7	2.2 ± 0.6
C[b]	10	JR-CSF	untreated	320 ± 92	100 ± 29	5.0 ± 0.26	17 ± 3.4	39 ± 11	12 ± 2.8	14 ± 3.7	1.0 ± 0.1	13 ± 2.6	2.8 ± 0.8
D	10	medium	–	negative	0.0 ± 0.0	negative	73 ± 1.6***	89 ± 0.5***	6.4 ± 0.4	1.3 ± 0.1***	5.2 ± 0.33***	170 ± 37***	130 ± 29***

Mice were infected intrathymically with HIV-1 JR-CSF at 26 weeks post-engraftment (top) and at 19 weeks post-engraftment (bottom). Six weeks post-infection with HIV-1 JR-CSF SCID-hu mice were treated with 300 μg of anti-CD47 three times a week for 3 weeks and compared to IgG-treated controls and untreated mice. Antiviral efficacy was evaluated by branched DNA assay to measure HIV-1 RNA and by ELISA to measure HIV-1 antigen p24. Thymocyte protection was evaluated by FACS analysis of Thy/Liv implant thymocytes using antibodies for HLA-ABC, CD3, CD4, and CD8. Data shown are mean ± SEM. *,**,***$p < 0.050$ was compared across indicated experimental groups by Mann-Whitney U test.

*$p \leq 0.050$ compared to untreated JR-CSF-infected mice (group C) by Mann-Whitney U test;

**$p \leq 0.050$ control Ab-treated JR-CSF-infected mice (group B) compared to anti-CD47 treated JR-CSF-infected mice (group A) by Mann-Whitney U test.

***$p \leq 0.050$ compared to untreated JR-CSF-infected mice (group C) by Mann-Whitney U test.

[a]Group B: mouse excluded from analyses (whole-body lymphoma); group D: mouse implant excluded from analyses (abnormal cell profile).

[b]Group B: two mice died (thymic lymphoma and cause unknown); group D: mouse died (cause unknown).

KEY RESOURCES TABLE

REAGENT or RESOURCE	SOURCE	IDENTIFIER
Antibodies		
anti-CD47 (Clone 410)	Bio X Cell	Cat#: BE0283
Isotype (rat IgG2a isotype)	Bio X Cell	Cat #. BE0089
anti-CD8 depleting antibody	Bio X Cell	Cat #. BE0061
anti-CD4 depleting antibody	Bio X Cell	Cat #. BE0003-1
Anti-CD8a	Thermo Fisher	Cat #25-0081-82
Anti-CD19	Thermo Fisher	Cat #25-0193-82
Anti-NK1.1	Thermo Fisher	Cat # 25-5941-81
Anti-CD4	Thermo Fisher	Cat #12-0041-82
Anti-CD11c	Thermo Fisher	Cat #25-0114-82
Anti-MHC class II	Thermo Fisher	Cat #11-5321-82
Anti-F4/80	Thermo Fisher	Cat #17-4801-82
Anti-CD107a	Thermo Fisher	Cat #12-1071-82
Anti-CD80	Thermo Fisher	Cat #11-0801-82
Anti-CD11b	BD Bioscience	Cat #11-0112-81
Anti-CD44	BD Bioscience	Cat #17-0441-82
Anti-CD86	BD Bioscience	Cat #12-0862-82
Anti-IFNγ	eBioscience	Cat #17-7311-82
Anti-TNF	eBioscience	Cat #11-7321-82
anti-LCMV-NP antibody	In house (self-made)	N/A
$CD8^+$ T cell isolation kit	Miltenyi Biotec	Cat #130-104-075
Tetramer (GP33/H-2Db)	Provided by the Tetramer Facility of the National Institutes of Health (NIH; Bethesda, MD, USA)	N/A
Synagis (anti-RSV monoclonal used as control Ab) in the second SCID-hu mouse study	Medimmune	N/A
APC-eFluor 780-conjugated anti-CD3	eBiosciences	Cat# 47-0038
PE-CY7-conjugated anti-CD4	BD Biosciences	Cat# 348789
PE-CY5.5-conjugated anti-CD8	Invitrogen	Cat#MHCD0818
Bacterial and Virus Strains		
LCMV-WE virus stock	Originally obtained from Prof. F. Lehmann-Grube, Heinrich Pette Institute, Hamburg, Germany) (Lehmann-Grube, 1971)	N/A
HIV-1 JR-CSF infectious molecular clone (pYK-JRCSF)	NIH AIDS Reagent Program	Cat# 2708
Chemicals, Peptides, and Recombinant Proteins		
LCMV-GP33-specific peptide	PolyPeptide Laboratories, Strasbourg, France	N/A
VSV-P52 peptide	PolyPeptide Laboratories, Strasbourg, France	N/A
diphtheria toxin	Sigma Aldrich	Cat #. MFCD00163490
Clodronate liposomes	Liposoma	SKU: CI-005-005
Experimental Models: Cell Lines		
MC57 cells	obtained from by the Ontario Cancer Institute, Canada	N/A

REAGENT or RESOURCE	SOURCE	IDENTIFIER
HEK293T/17 cells	ATCC	Cat# CRL-11268
Experimental Models: Organisms/Strains		
C57BL/6J mice	Jackson Laboratories	JAX000664
Sirpa mice	Riken Bioresource Center	RBRC01544
$Tcrb^{tm1Mom}$/J (*TCRb*$^{-/-}$) mice	Jackson Laboratories	JAX002118
CD11c-DTRtg mice	Prof. Phillip Lang's lab at the Heinrich-Heine-University, Dusseldorf	N/A
P14.CD45.1 mice	Tak W. Mak at the Campbell Family Cancer Research Institute and University Health Network, Toronto, Canada	N/A
C.B-17 SCID (C.B-*Igh-1b*/IcrTac-*Prkdc*^{scid}) mice	Taconic	Cat# CB17SC-M
Software and Algorithms		
FlowJo software	FlowJo LLC, Ashland, OR, USA	N/A
StatView 5.0	Abacus Concepts	N/A